Mechanism of Adenosine Triphosphate Hydrolysis by Actomyosin*

R. W. Lymn and E. W. Taylor†

ABSTRACT: The hydrolysis of ATP by acto-HMM has been studied during the transient state using a rapid-mixing apparatus. The rate of substrate binding was slightly slower and the rate of hydrolysis of the first molecule of ATP was essentially the same as for heavy meromyosin (HMM) alone. The rate of acto-HMM dissociation after binding substrate was too fast to measure in a stopped-flow apparatus, consequently dissociation occurs before hydrolysis of the bound ATP. By means of a rapid column separation procedure it was shown that actin combines with the myosin·ADP·P complex and displaces the products of the hydrolysis reaction. It is concluded that this step is responsible for activation of myosin ATPase by actin. A simple kinetic scheme which accounts for the transient and steady-state behavior is presented and compared with the contraction cycle postulated for the sliding filament mechanism.

Under physiological conditions, namely, 0.1–0.15 M KCl and greater than 1 mM $MgCl_2$, myosin ATPase activity is strongly inhibited. Natural or synthetic actomyosin under these same conditions exists as a precipitate. Addition of ATP usually leads to "clearing," a decrease in turbidity of the system, which is indicative of dissociation of actin and myosin, at least as measured by physical methods such a flow birefringence or viscosity (Maruyama and Gergely, 1962). The ATPase activity in the clear phase is only slightly higher than that of myosin ATPase. As long as traces of Ca ions are present this phase is followed by precipitation and superprecipitation and a 10- to 20-fold increase in ATPase activity. Although this activation is clearly related to the mechanism of contraction, a heterogeneous system is unsuitable for kinetic studies.

A better understanding is obtained from studies of the heavy meromyosin–actin complex which remains essentially homogeneous and does not superprecipitate. The fundamental work of Eisenberg and Moos (1968, 1970; Eisenberg *et al.*, 1969) has considerably clarified our understanding of this system. Two competing reactions are involved, the dissociation of actomyosin by ATP and the activation of myosin ATPase by actin. Analysis of the steady-state kinetics by Eisenberg and Moos showed that the behavior could be interpreted as a decrease in the HMM–actin association constant when ATP is bound and a large increase in actin-HMM ATPase relative to myosin. By interpreting the kinetics by a modified Michaeles–Menten scheme, the corresponding association and steady-state rate constants were obtained by extrapolating to infinite actin concentration. The real rate of the activated enzyme was found to be about 200 times larger than for myosin.

The scheme could be formulated as

$$\begin{array}{ccccc} AM + ATP & \rightleftharpoons & A\cdot M\cdot ATP & \xrightarrow{20\ sec^{-1}} & AM + ADP + P \\ & {\scriptstyle +A}\uparrow\downarrow{\scriptstyle -A} & & & \\ M + ATP & \rightleftharpoons & M\cdot ATP & \xrightarrow{0.1\ sec^{-1}} & M + ADP + P \end{array}$$

In this scheme hydrolysis occurs largely through the AM·ATP state. Recent studies on the transient state of ATP hydrolysis by myosin and HMM (Lymn and Taylor, 1970) have shown that the first mole of ATP is hydrolyzed at a rapid rate, roughly 100 sec^{-1}, which is much faster than the maximum rate in the Eisenberg and Moos mechanism under comparable conditions. The slow steady-state rate for myosin ATPase was attributed to the rate-limiting dissociation of the products, ADP, and phosphate from the enzyme (Taylor *et al.*, 1970). These studies therefore suggested a modified view of the actin activation mechanism in which actin might affect the rate of product dissociation rather than the hydrolytic step itself.

The work presented here describes a study of the HMM–actin system in the transient state. A provisional and no doubt oversimplified mechanism is proposed which is consistent with the transient state experiments as well as the steady-state studies of Eisenberg and Moos. The essential feastures of the mechanism are that actomyosin dissociation preceeds hydrolysis, and activation is produced by recombination of actin with the myosin–products complex with displacement of products. The steps in the mechanism can be identified with the contractile cycle postulated in the sliding filament model (Huxley, 1968; Pringle, 1967).

Materials and Methods

Proteins. Rabbit myosin and heavy meromyosin (HMM)[1] were prepared as described previously (Finlayson *et al.*, 1969). Acetone powder was prepared by the method of Tonomura and Yoshimura (1962) and actin was extracted from the powder at 0° by the method of Carsten and Mommaerts (1963).

Concentrations of HMM and actin were determined using the difference in absorbance at 291 and 350 mμ in 0.5 N NaOH ($\epsilon_{251} - \epsilon_{350}$ = 776 cm^2/g for HMM; $\epsilon_{291} - \epsilon_{350}$ = 1150 cm^2/g for actin). These figures were obtained by micro-Kjeldahl analyses assuming a nitrogen content of 16.7%. For the calculations in this paper the molecular weights of HMM and actin are assumed to be 350,000 and 50,000, respectively.

ATPase Measurements. The early phase of ATP hydrolysis was measured by determination of [^{32}P]phosphate libera-

* From the Department of Biophysics, University of Chicago, Chicago, Illinois 60637. *Received July 8, 1971.* This work was supported by National Institutes of Health, Grant No. GM 1992, Muscular Dystrophy Association, and Life Insurance Medical Research Fund. E. W. T. acknowledges a Research Career Development award from the U. S. Public Health Service; R. W. L. acknowledges support from the U. S. Public Health Service Training Grant GM 780.

† To whom to address correspondence.

[1] Abbreviation used is: HMM, heavy meromyosin.

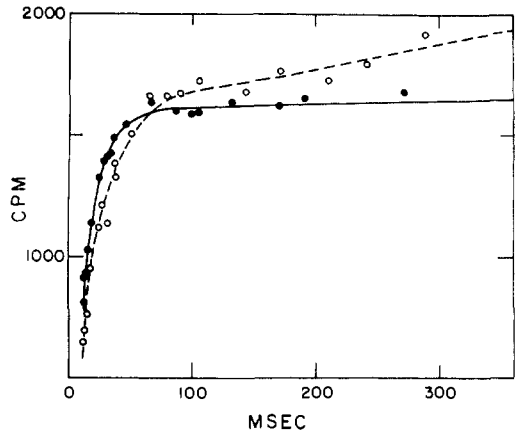

FIGURE 1: Early phase in the hydrolysis of ATP by HMM and acto-HMM. (●) Phosphate liberation by HMM, (○) phosphate liberation by acto-HMM. Conditions 0.05 M KCl–0.02 M Tris buffer (pH 8), 20°, 5×10^{-3} M $MgCl_2$, 25 mM ATP, 4.8 moles of actin/mole of HMM, and 1 mg/ml of HMM. Intercept of the linear portion corresponds to an early burst of approximately 1.1 moles of phosphate/mole of HMM.

tion from [γ-^{32}P]ATP employing the chemical-quench flow apparatus described previously (Lymn and Taylor, 1970). The dissociation of actomyosin was determined from measurements of turbidity in the stop-flow spectrophotometer employed in previous experiments (Finlayson *et al.*, 1969). The use of rate turbidity change as a measure of rate of actomyosin dissociation has been discussed (Finlayson *et al.*, 1969) and it was concluded that the rate constant should be correct within a factor of 2. With HMM–actin the accuracy should be somewhat improved since the difference in the scattering factors of actin and acto-HMM is smaller than for the actin–myosin system.

A technique for measurement of rate of dissociation of reaction products, ADP, and phosphate from the enzyme complex has been described (Taylor *et al.*, 1970). In the former work it was shown that myosin could be separated from unreacted substrate by rapid filtration on a 6- to 8-cm column of G-25 fine Sephadex. Separation was accomplished in times as short as 30–40 sec. In the present work we wished to determine the effect of addition of actin to a myosin–products complex. A simple three-compartment mixing device (*loc cit.*) was used and its operation is best described by giving the details of a typical experiment. Myosin (0.25 ml, 10^{-5} M) and [^{3}H,γ-^{32}P]ATP (0.25 ml, 2×10^{-5} M) in 2% sucrose and the appropriate buffer were added as a layer under a column of buffer in chambers 1 and 2. The cross-sectional area of the third chamber was the sum of the areas of chambers 1 and 2. It contained a layer of 0.75–1.25 ml of the component to be mixed, *i.e.*, actin or buffer. Pistons were depressed by a block driven by translation of a screw (a modified furniture clamp). Solutions 1 and 2 were mixed in a simple T-mixer, traversed a short loop of polypropylene tubing, and were mixed with solution 3. The time delay to traverse the loop was the order of 1 sec. The mixture passed into a modified chromatography column filled to the top with Sephadex G-25. The column was constructed from Lucite plus standard fittings for a Glenco column. A baffle plate replaced the usual inlet connection to spread the solution more evenly across the top of the resin bed. Although the dead volume from mixer to resin bed was kept as small as possible some compression of resin bed could not be avoided at the pressures employed. When the mixture had entered the column, a three-way stop cock was turned to allow fluid flow from a buffer reservoir driven by a Harvard apparatus pump. The column and buffer were thermostated by circulating water from a temperature bath.

Resolution was somewhat poorer than with the technique previously employed of successive layering on top of the resin bed but was adequate for separation of the enzyme–product complex and permitted successive mixing of substrate and actin with the myosin solution.

Results

The transient phase in the hydrolysis of ATP by acto-HMM was measured at low ionic strength for a range of actin concentrations which gave an appreciable activation of the steady-state rate of hydrolysis.

A typical experiment is shown in Figure 1 (0.05 M KCl, 0.02 M Tris buffer, 5×10^{-3} M $MgCl_2$, and 25 μM ATP, pH 8, 20°). The solid circles refer to phosphate production by HMM alone and show the typical early burst of slightly more than 1 mole/mole. On this time scale the steady-state rate differs but little from a horizontal line, and is reached in less than 100 msec at this ATP concentration.

The open circles are for acto-HMM (4.8 moles of actin/mole of HMM). Three aspects of the curve should be noted. The steady state is reached after nearly the same interval of time but the steady-state rate is considerably larger (a factor of at least tenfold). During the transient phase the rate of hydrolysis is actually slightly less. As described below, this result shows that the apparent rate constant for substrate binding to acto-HMM is less than for HMM. Finally, the size of the early burst is essentially unchanged.

The data were analyzed in the manner described previously (Lymn and Taylor, 1970). The contribution from the steady state was subtracted by extrapolation of the linear region to zero time. A semilog plot of the difference fitted a straight line, indicating that the transient process could be fitted adequately by a single rate constant. In the present example, the rate constant was 65 sec^{-1} for HMM alone and 50 sec^{-1} for acto-HMM. The steady-state rates were 0.08 and 0.9 sec^{-1}, respectively. At the low ionic strength which had to be employed to obtain appreciable activation, the transient rate is quite large and any small deviation from a linear log plot during the earliest part of the transient state would not have been detectable.

The effect of varying actin was measured at a particular substrate concentration, 25 μM ATP (Figure 2). The presteady-state rate constant determined from semilog plots decreased sharply with increasing actin concentrations and reached a plateau at a ratio of 0.4 g of actin/g of HMM, or a molar ratio of approximately 3 actins/HMM. In various assays (viscosity, turbidity), 2 or 3 actins per myosin are usually required to saturate myosin binding sites (Finlayson *et al.*, 1969). The results indicate that the apparent substrate binding rate constant is somewhat lower for acto-HMM than for HMM and is not further reduced by excess actin.

The variation in rate constant as a function of substrate concentration is shown in Figure 3. The upper curve is for HMM alone. The apparent rate constant increases with substrate concentration, finally reaching a plateau. As discussed in previous work, the slope of the plot at low substrate concentrations gives the apparent second-order rate constant for substrate binding and the value at the plateau is the first-order rate constant for the hydrolytic step. With increasing concentrations of actin at each substrate concentration, the

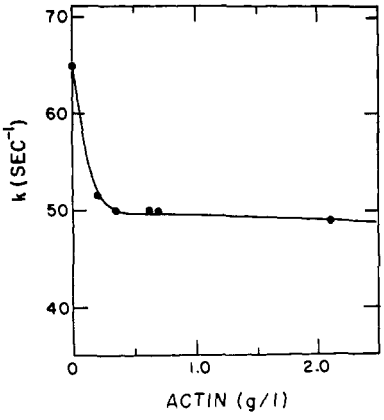

FIGURE 2: Dependence of rate constant of the early phase of phosphate production on actin concentrations at a constant ATP concentration of 25 μM. Other conditions as in Figure 1, 1 mg/ml of HMM.

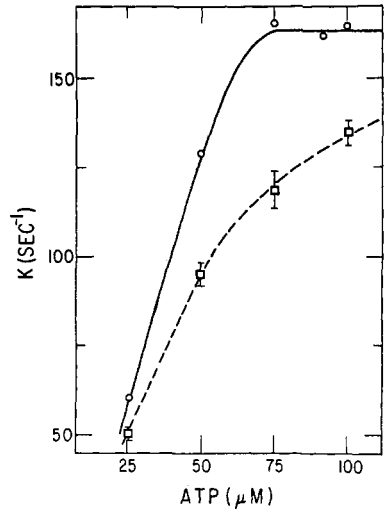

FIGURE 3: Presteady-state rate of phosphate production by HMM and acto-HMM, 0.05 M KCl, 5×10^{-3} $MgCl_2$, pH 8, 20°, (○) HMM, (□) acto-HMM. For each substrate concentration the rate constant was determined for two or more actin to HMM ratios in the range from 0.4 to 2.16 actin to HMM by weight. There was no significant variation with actin to HMM ratio, and data were averaged for each substrate concentration. Standard deviations are indicated by the error bars. The points are average values of 13 experiments.

apparent presteady-state rate constant decreased as HMM is replaced by acto-HMM, and the value at high actin concentration corresponds to acto-HMM. The lower curve refers to actin to HMM weight ratios of 0.4 or larger, for which the sites should be nearly or completely saturated with actin. Over the lower range of substrate concentrations the slope is less than for HMM, the values of the second-order rate constants being approximately 1.8×10^6 M^{-1} sec^{-1} for acto-HMM *vs.* 2.4×10^6 M^{-1} sec^{-1} for HMM.

Because of the lower slope, a plateau was not reached in the accessable concentration range. The data are also rather scattered partly because it was necessary to combine results from different preparations. However, it is clear that the rate does not increase linearly with substrate concentration above 50 μM ATP and appears to be approaching a plateau which is probably not larger than for HMM alone. The value could not be accurately determined but is the order of 100–150 sec^{-1}.

Rates of this magnitude are difficult to measure in the mixing apparatus since the transient phase is three-quarters complete at the earliest time point that can be measured.

Dissociation of Acto-HMM. Mixing of ATP and acto-HMM leads to dissociation of the protein complex. A crucial question is whether the acto-HMM–ATP complex dissociates before or after the ATP is hydrolyzed. This question could be answered by measuring the first-order rate constants for bond hydrolysis and for dissociation, steps 2 and 3, respectively.

$$\begin{array}{ccccc} AM + ATP & \overset{1}{\rightleftharpoons} & AM\cdot ATP & \overset{2}{\rightleftharpoons} & AM\cdot ADP\cdot P \\ & & \Updownarrow 3 & & \\ & & A + M\cdot ATP & & \end{array}$$

The experiments described in the last section provide an estimate of the rate for the hydrolysis step. In principle, step 3, the dissociation step, could be measured by determining the rate of turbidity change as a function of ATP concentration, if a maximum rate is reached at high ATP concentrations. In a previous study with actomyosin in 0.5 M KCl (Finlayson *et al.*, 1969), the rate of dissociation for a given ATP concentration fitted a single exponential step, but the rate was a linear function of ATP concentration up to rates of 250 sec^{-1}. Thus the rate for step 3 is considerably larger than 250 sec^{-1} under these conditions.

Similar experiments were performed for acto-HMM under the same conditions as were used in the phosphate production experiments. Oscilloscope traces illustrating the turbidity change are shown in Figure 4. Semilog plots of the turbidity change fitted a single exponential. The rate constant for dissociation increased linearly with ATP concentration to values which were too fast to be accurately measured. A plot of rate constant *vs.* concentration is shown in Figure 5. The slope gives a second-order rate constant of 1.2×10^6 M^{-1} sec^{-1} which agrees approximately with the rate constant for substrate binding determined from ATP hydrolysis.

The apparent rate constants of dissociation showed no sign of reaching a plateau, which implies that the actual rate constant of dissociation is much larger than the largest number measured. The dissociation reaction was investigated at a higher ionic strength (0.1 M KCl) and a lower temperature (10°) in order to slow down the reaction. Under these conditions the maximum rate of the hydrolytic step is less than 50 sec^{-1}. The traces shown in Figure 4a,b are from one such experiment. Raising the ATP concentration 50-fold from 10^{-5} to 5×10^{-4} M increased the rate by a factor of about 50-fold. At the higher concentration the half-life is less than 10 msec. As concentration is raised further the rate constant continues to increase becoming too large to measure. The third trace in the figure is from an experiment at 10^{-2} M ATP and 20°. The turbidity falls to the final value shortly after flow begins, consequently the reaction is completed during the transit time from the mixer to the observation window which is about 3 msec. The rate of dissociation is too fast to measure by the stopped-flow method and the actual rate constant is 1000 sec^{-1} or larger.

Product Dissociation. Under conditions in which actin increases the steady-state rate of hydrolysis more than tenfold, the kinetic evidence indicates that hydrolysis of substrate occurs after dissociation of the actin. The simplest explanation

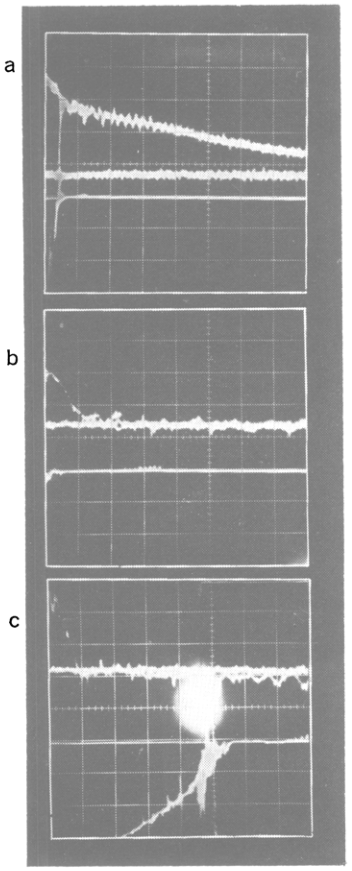

FIGURE 4: Dissociation of acto-HMM induced by ATP. (a) 10^{-5} M ATP, 5×10^{-3} M $MgCl_2$, 0.1 M KCl, 0.05 M Tris buffer, pH 8, 5×10^{-6} M HMM, 2.5×10^{-5} M actin, 10°; time scale 100 msec/major division. The lower trace is a signal monitoring the position of the drive block. Flow stops at about 50 msec after the beginning of the sweep. A second sweep a few seconds later gave the thick horizontal line indicating the final turbidity. The half-life of the turbidity change is 450 msec. (b) Conditions as in part a except the ATP concentration was 5×10^{-4} M; time scale 10 msec/major division. Flow stops approximately 2 msec after the beginning of the sweep. The half-life is approximately 7 msec. (c) 10^{-2} M ATP, 1.5×10^{-2} M $MgCl_2$, 20°, other conditions as in part a. Time scale 20 msec/major division. Sweep was triggered at the beginning of the drive. Rising trace indicates the position of the drive block. Flow stops near the middle of the trace. The turbidity falls to the final value long before the flow stops, indicating reaction is complete before solution reaches the observation chamber, which requires 3 msec. The light area af the center of the figure is a reflection from room lights.

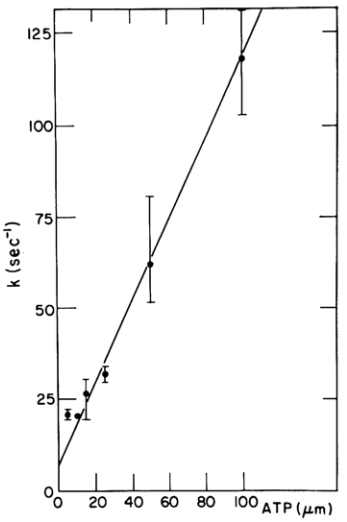

FIGURE 5: Dependence of the rate of dissociation of acto-HMM on ATP concentration. 0.05 M KCl, 5×10^{-3} M $MgCl_2$, pH 8, 20°, 3.5 moles of actin/mole of HMM, and 5.7 μM HMM. Solid circles are average values of at least two determinations; error bars indicate the range of values for a given concentration. At the lowest concentration of 5 μM the apparent rate of dissociation is not expected to be simply related to ATP concentration since dissociation is incomplete and ATP concentration is not constant.

of this activation is that actin recombines with the myosin–product complex and displaces the products

$$M \cdot ADP \cdot P + A \rightleftharpoons AM \cdot ADP \cdot P \longrightarrow AM + ADP + P$$

The ability of actin to increase the rate of product dissociation was demonstrated by use of the rapid column separation procedure. HMM was mixed with [^{3}H,γ-^{32}P]ATP as described in Materials and Methods section and then, after about 1–2 sec, it was further mixed either with unlabeled ATP or with actin plus unlabeled ATP. The protein peak was separated from free nucleotides and phosphate by rapid elution from a Sephadex G-25 column and assayed for bound ADP and phosphate. The column buffer also contained unlabeled ATP, ADP, and phosphate.

The experimental conditions were chosen to simulate the final two steps in the mechanism. At a concentration of $1–2 \times 10^{-5}$ M ATP the M–ATP complex forms in 0.1–0.2 sec and is then converted to M·ADP·P in 0.1–0.2 sec. The latter complex decays with a half-life of about 30–50 sec at a temperature of 5°. Consequently the M·ADP·P complex will be formed during transit between mixers and can react with actin in the second mixer. Further binding of label is prevented by a 50- to 100-fold excess of unlabeled ATP, present with the actin. The behavior of the labeled complex can be followed on the column and any back-reactions are suppressed by excess unlabeled ATP, ADP, and phosphate in the column buffer.

Experiments were performed with HMM and myosin at a variety of ionic strengths. It was possible to work with myosin at an ionic strength of 0.1 M KCl for the column buffer since the high ATP concentration keeps actin and myosin essentially dissociated.

An experiment in 0.1 M KCl is shown in Figure 6a. In the absence of actin, a label peak of ADP and phosphate elutes with myosin. The half-life of the M·ADP·P complex was about 50 sec^{-1}. When mixed with actin under the same conditions, there is a barely detectable shoulder at the position of the protein peak indicating a half-life shorter by a factor of at least five.

The experiment is easier to perform at a higher ionic strength (0.3 M KCl). Although actin activation is reduced at this ionic strength, the slower decay of the myosin–product complex allows a much larger binding of products in the control (Figure 6b). In this experiment we have plotted total ^{3}H or ^{32}P counts, but on the protein peak, these correspond to ADP and phosphate. There is at least a tenfold decrease in bound products.

A similar and quantitatively more striking result is obtained with pyrophosphate (Figure 6c). In this case pyrophosphate is preincubated with HMM and then mixed with actin and eluted. In the control there is very little dissociation of pyrophosphate from HMM at 0° in the time necessary to elute the protein. When mixed with actin, the bound pyrophosphate is completely displaced.

Finally, experiments were also performed in which [^{3}H]-

ADP or [^{3}H]ADP, and [^{32}P]phosphate were incubated with myosin and then mixed with actin. Again it was found that actin displaces ADP and the small amount of phosphate which was bound.

Discussion

This series of experiments establishes some general features of the mechanism of ATP hydrolysis by acto-HMM. The main results are: (a) an early burst of ATP hydrolysis of approximately the same magnitude and with similar values for the rate constants as for HMM alone; (b) dissociation of acto-HMM as measured by turbidity change occurs by a very fast step following ATP binding. The actual rate of this step is too fast to measure by stop-flow methods and is at least ten times larger than the rate of splitting of ATP, consequently the system largely dissociates into A + M·ATP; (c) the step in which ATP is hydrolyzed must occur predominantly on the free myosin, M·ATP → M·ADP·P; and (d) actin can react with the myosin–product complex causing the products to be released at a much faster rate than from myosin alone. Actin activation of myosin ATPase therefore occurs at the product release step and not at the ATP hydrolysis step.

The following kinetic scheme accounts for the experimental results

$$\begin{array}{ccccc} \mathrm{AM} + \mathrm{ATP} & \overset{4}{\rightleftharpoons} & \mathrm{AM{\cdot}ATP} & \overset{7}{\rightleftharpoons} & \mathrm{AM{\cdot}ADP{\cdot}P} \rightleftharpoons \mathrm{AM} + \mathrm{ADP} \\ & & 5\Big\downarrow\Big\uparrow(-\mathrm{A}) & & 6\Big\downarrow\Big\uparrow(+\mathrm{A}) \qquad + \mathrm{P} \\ \mathrm{M} + \mathrm{ATP} & \overset{1}{\rightleftharpoons} & \mathrm{M{\cdot}ATP} & \overset{2}{\rightleftharpoons} & \mathrm{M{\cdot}ADP{\cdot}P} \overset{3}{\rightleftharpoons} \mathrm{M} + \mathrm{ADP} + \mathrm{P} \end{array} \qquad (1)$$

For each step there are a pair of rate constants k_i and k_{-i} numbered as indicated by eq 1. A rough set of values for the forward rate constants for 0.05–0.1 M KCl, pH 8, 20° is as given: k_1, 2×10^6 M^{-1} sec^{-1}; k_2, 100–150 sec^{-1}; k_3, 0.05 sec^{-1}; k_4, 1×10^6 M^{-1} sec^{-1}; k_5, $\geqq 1000$ sec^{-1}; k_6, 3×10^5 M^{-1} sec^{-1}; and k_7, 10–20 sec^{-1}. The scheme is the simplest that will account for the main experimental findings; we recognize that the scheme is incomplete but the available evidence does not warrant a more complicated scheme. In particular, there may be other intermediate states in the hydrolytic process (step 2); nothing can be said about the very important question of configuration changes accompanying the binding or splitting of substrate or the dissociation of products. An important criticism is that myosin has two hydrolytic sites and we have ignored any effects which may arise through interactions between sites. Nevertheless the scheme calls attention to what appear to be essential features of the mechanism and we wish to discuss the experimental evidence for the various steps.

The dependence of the rate of the early burst on substrate concentration shows that the rate constant for substrate binding to acto-HMM is smaller than for HMM. This suggests that the presence of actin exerts some interaction with the catalytic site which reduces the rate at which ATP binds.

A systematic study of the size of the early burst was not made, except to note that at various ATP concentrations the early burst for acto-HMM was equal to that of HMM alone. The size of the burst increased slightly with ATP concentration in the range 25–100 μM but was less than 1.5 moles/mole. In previous work with myosin and HMM (Lymn and Taylor, 1970) the size of the early burst did not show a simple dependence on ATP concentration, and could not be correlated with a Michaelis constant of 10^{-6} M. It is possible that the two sites of HMM are not equivalent, but we prefer not to speculate on this point until studies are completed with subfragment one. Under the conditions of the quench-flow experiments the majority of the HMM molecues contained only one molecule of products. It is not known whether the second site is empty or occupied by a molecule of ATP.

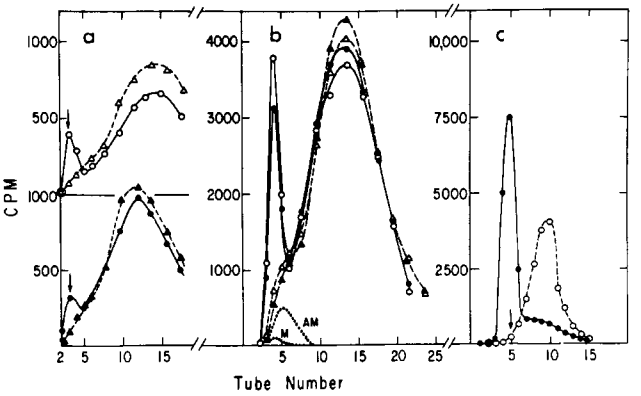

FIGURE 6: (a) Dissociation of myosin–product complex by actin. Conditions: 0.1 M KCl, 8°, 0.05 M Tris buffer, pH 8, 5×10^{-3} M $MgCl_2$, 0.25 ml of myosin (3.5×10^{-5} M) mixed with 0.25 ml of [^{3}H,^{32}P]ATP (2×10^{-5} M) and further mixed after 1–2 sec with 1 ml of actin (7×10^{-5} M) plus unlabeled ATP (10^{-3} M) (- - -) or ATP alone (—). Protein peak, indicated by arrow, eluted at approximately 40 sec after mixing. Column buffer contained 10^{-3} M ATP and phosphate. Fractions of 3 ml were collected in tubes containing perchloric acid and carrier ATP, ADP, and phosphate, and each tube was assayed for ADP and phosphate. (●) Phosphate, no actin; (○) ADP, no actin; (▲) phosphate, actin present; (△) ADP, actin present. (b) Dissociation of myosin product complex by actin. Conditions 0.3 M KCl, 7°, 0.05 Tris buffer, pH 8, 5×10^{-3} M $MgCl_2$. Myosin (0.25 ml; 1.8×10^{-5} M) mixed with 0.25 ml of [^{3}H,^{32}P]-ATP (2×10^{-5} M) and further mixed with 1 ml of 6×10^{-5} M actin plus 10^{-3} M ATP (- - -) or ATP alone (—); 3 ml/tube, protein peak eluted at 45 sec (no actin) and 50 sec (plus actin). (●) ^{32}P, no actin; (○) ^{3}H, no actin; (▲) ^{32}P, actin present; (△) ^{3}H, actin present. Positions of protein peaks determined by absorpton at 276 nm are given by dotted curves; M and AM refer to myosin and actomyosin, respectively. (c) Dissociation of myosin–pyrophosphate complex by actin. HMM (10^{-5} M) incubated 30 min with pyrophosphate (10^{-5} M) in 0.05 M KCl, 0.5 M Tris buffer, pH 8, 2×10^{-3} M $MgCl_2$, 5°. 0.8 ml mixed with 1.5 ml of actin (4×10^{-5} M) plus 10^{-3} M unlabeled pyrophosphate (○) or pyrophosphate alone (●); column buffer contained 10^{-3} M pyrophosphate. Protein peak indicated by the arrow eluted 60 sec after mixing.

Turbidity measurements showed that actin dissociates following ATP binding at a rate which is too fast to measure (k_5) and which is much larger than the hydrolysis step (k_2). Objections can be raised to the use of turbidity as a measure of dissociation (we have discussed this point previously (Finlayson *et al.*, 1969)) and it can also be asked whether the turbidity change is due to dissociation of the HMM or to some other change in the state of aggregation of the system. In this series of experiments and in earlier work with actomyosin the rate of the turbidity change did not depend on the actomyosin concentration or on the myosin to actin ratio. It is therefore unlikely that the turbidity change is due to dissociation of large aggregates formed by actin–actin or myosin–myosin interactions. The turbidity change is fitted by a single rate constant until the final turbidity is reached. As this turbidity is the sum of the turbidities of actin and myosin and the system appears to be dissociated by physical measurements (sedimentation, viscosity, and flow birefringence), there is no evidence to support a two-step process.

It can be asked whether one or two molecules of ATP must

be bound to cause dissociation. The experimental evidence for actomyosin at high ionic strength (Finlayson *et al.*, 1969) and acto-HMM at low ionic strength favors binding of a single ATP since the turbidity change could be fitted by a single exponential term. If two ATP molecules have to bind and the rate constants for binding are different, then it is easily proven that the turbidity change should fit two exponential terms and show an early lag. This type of behavior was not found except in the presence of a high Ca concentration at 0° (Finlayson *et al.*, 1969) which is not a physiological state. If the rate constants for binding of ATP are identical then turbidity change would take the form $(1 + kSt)e^{-kSt}$, where k is the apparent rate constant for binding and S is the ATP concentration. In this case turbidity change would not fit an exponential and at short times, such that $kSt \ll 1$, the rate of dissociation would be proportional to S^2. For a variety of reagents the rate of dissociation was always proportional to S.

The rate of the hydrolytic step is given by the maximum rate of the early burst at high substrate concentrations. Since the system dissociates before hydrolysis, this rate should be the same as for HMM alone. The maximum rate was not reached in the accessible substrate concentration range (Figure 3) because of the lower rate constant for substrate binding but the curve appears to be reaching a plateau which is not larger than the value for HMM. Since $k_5 \gg k_2$, the rate of hydrolysis of ATP on the AM is unknown as it did not contribute appreciably to the measured hydrolysis. However, we can rule out the possibility that it is very large and comparable to k_5 (the assumption implicit in the mechanism of Eisenberg and Moos) since in that case the apparent rate of the early burst would have increased linearly with substrate concentration over the whole range.

The scheme requires that steps 6 and 7, the recombination of actin with the myosin–products complex and the dissociation of products, occur at a reasonable rate. The maximum rate of hydrolysis at infinite actin concentration must correspond either to k_2 or k_7, whichever is smaller. Since the maximum rate obtained by Eisenberg and Moos, under comparable conditions, is 10–20 sec^{-1} and k_2 is the order of 100 sec^{-1}, k_7 can be identified with the maximum rate. k_6 has not been directly measured but an estimate is obtained by measuring the rate of turbidity change when myosin–ADP is mixed with actin. A preliminary figure is 3×10^5 M^{-1} sec^{-1} in 0.1 M KCl. This value is large enough to account for actin activation.

It seemed necessary to demonstrate in a more direct way that interaction with actin would increase the rate of release of products. The rapid column separation technique clearly showed that the life time of the product complex was reduced at least by a factor of ten by combination with actin. However, it should be stressed that this is a minimum estimate and these experiments are not a measurement of k_7. The lifetime of the AM·ADP·P complex is expected to be less than 0.1 sec, while 30–50 sec are required to elute the column. The rate-limiting step is the combination of actin with the myosin–product complex and radioactivity remaining bound to protein is a measure of the extent to which this step did not occur during the time necessary to eluate the column plus any errors arising from incomplete mixing.

The column experiments were performed over a range of ionic strengths from 0.1 to 0.3 M in KCl and even at the highest ionic strength displacement of products was nearly complete (Figure 6b). This may at first appear surprising since actin gives only a slight activation of the myosin ATPase at this ionic strength. As shown by Eisenberg and Moos (1970) k_7, the product dissociation step is relatively independent of ionic strength. Low activation is due to a decrease in the association constant for the binding of actin to the myosin–product complex. In the column experiments we still expect product dissociation to occur as long as actin binds to the myosin–product complex at least once in the 30 sec needed to elute the column.

The kinetic scheme was deduced from transient-state measurements and it is necessary to show that it accounts for the steady-state behavior and yields the same values of the Michaelis constants found by Eisenberg and Moos. The steady-state experiments require a linear relationship between the reciprocal of the rate of hydrolysis and the reciprocal of the actin concentration. At a moderate ATP concentration (10^{-4} M), the rates for steps 4, 5, and 2 are 100 sec^{-1} or larger while the steady-state rate is the order of 10 sec^{-1}. Since AM would be converted to M·ADP·P as fast as it is formed, the mechanism can be divided into two parts:

$$\mathrm{M\cdot ADP\cdot P + A} \overset{k_6}{\rightleftharpoons} \mathrm{AM\cdot ADP\cdot P} \xrightarrow{k_7} \mathrm{AM + ADP + P}$$

$$\mathrm{AM + ATP} \xrightarrow{\text{fast}} \mathrm{M\cdot ADP\cdot P + A}$$

The steady-state rate is therefore determined by the first line and it is obvious that the equation has the form of a Michaelis–Menten mechanism and must yield a linear double-reciprocal plot. Furthermore, denoting the Michaelis constant by K_M

$$K_M^{-1} = \frac{k_6}{k_{-6} + k_7}$$

Eisenberg and Moos have interpreted this constant as the AM·ATP dissociation constant. In our scheme, it must refer to the product complex AM·ADP·P, though it need not be a dissociation constant. K_M^{-1} is approximately 10^4 M^{-1} and k_7 is 10–20 sec^{-1}. These values require $k_6 \geqq 10^5$ M^{-1} sec^{-1}, and we have obtained an approximate value of 3×10^5 M^{-1} sec^{-1} for k_6. These arguments, though preliminary, suggest that k_{-6} is at most of the same order of magnitude as k_7, and K_M^{-1} is thus only a rough estimate of the equilibrium constant. By varying ATP at a high actin concentration Eisenberg and Moos (1970) obtained K_M^1, the Michaelis constant of the ATPase. In our scheme $(K_M^1)^{-1}$ is k_4/k_7. k_4 is approximately 1.5×10^6 M^{-1} sec^{-1} in 0.05 M KCl and since k_7 is 20 sec^{-1} we obtain a value of 0.8×10^5 M^{-1} which agrees with their value of 0.6×10^5 M^{-1}. However their value refers to very low ionic strength and was stated not to depend on ionic strength in the range from 10 to 20 mM in KCl. k_4 does vary with ionic strength in the range 0.05–0.5 M KCl by a factor of at least five and since k_7 is relatively independent of ionic strength we expect K_M^1 to depend on ionic strength. As we have not measured k_4 at very low ionic strength it is not clear whether this is a real discrepancy. It can be concluded that the scheme derived from transient-state studies is also in agreement with the steady-state measurements.

The mechanism stresses the importance of interaction between actin and the substrate or products in the various complexes. The changes in rate or equilibrium constants which lead to dissociation of actomyosin or activation of enzyme activity require an interaction between ATP or ADP and actin when both are bound to myosin. Either the separation between the respective binding sites is small enough to allow direct interaction between charges or binding of nucleotide alters the configuration at the actin site and conversely.

Dissociation of AM by ATP and activation of myosin ATPase by actin are aspects of the same reaction. This can be seen most clearly from the effect of pyrophosphate (PP) which is a nonhydrolyzable analog of the substrate or product. From

$$PP + AM \rightleftharpoons AM \cdot PP \rightleftharpoons A + MPP$$

left to right the reaction is the dissociation of AM by PP and from right to left, the displacement of PP by actin which is the analog of activation of the enzyme. Neither step depends on hydrolysis and the kinetics of both steps depends on an "interaction" of PP and actin when both are bound to myosin. Reduction of ADP or PP binding to myosin by actin has been described by Gergely *et al.* (1959) and Kiely and Martonosi (1968) based on equilibrium dialysis experiments.

Relation of Kinetic Scheme to Models of Muscle Contraction. The aim of enzyme kinetic studies is to provide a molecular mechanism and a quantitative model for the events which are presumed to take place in muscle contraction. A large body of evidence derived from electron microscopy and X-ray diffraction, has led to what may be called the sliding-filament–moving-bridge model (Huxley, 1968; Pringle, 1967). The cycle of events for a single bridge is shown in Figure 7a. The diagram is purposely schematic in that no attempt is made to draw a two-headed myosin structure or to indicate a possible hinge at the base of the molecule. The four steps in the cycle are: (1) the dissociation of the actin–bridge complex, (2) movement of the free myosin bridge, (3) recombination of the bridge with actin, and (4) the drive stroke. The four main steps in the enzyme mechanism are shown in Figure 7b. These steps are: (1) the binding of ATP and very rapid dissociation of actomyosin, (2) the splitting of ATP on the free myosin, (3) recombination of actin with the myosin-products complex, and (4) the displacement of products.

The similarities of the two schemes are obvious. Steps 1 and 3 in both schemes involve the dissociation and recombination of actin and myosin and it appears quite reasonable to identify the corresponding steps. The chemical mechanism provides an explanation of how a cycle involving dissociation and recombination of myosin bridges could be coupled to ATP hydrolysis. Also the myosin–product complex is a metastable state with a long half-life which can await the arrival of an actin unit in the proper orientation to allow interaction.

The question is how much further should one push the similarities. One might suppose that either the binding or the splitting of ATP induces a configuration change which accounts for movement of the free bridge (step 2). One might go even further and suppose that after formation of the AM·ADP·P complex, dissociation of products leaves the AM in a configuration, rather like a stretched spring so that tension is exerted or movement is produced in returning to the original configuration (step 4).

This interpretation is not unreasonable and makes use of the popular notion that the binding of a small molecule is capable of altering the configuration of a protein. However, our kinetic studies provide no evidence for a large change in the configuration of myosin associated with ATP binding or hydrolysis. Furthermore there is no evidence for a large-scale change of shape of myosin in solution (Gratzer and Lowey, 1969) and there is no kinetic evidence of any kind for a configuration change that could be identified with a step in the contraction cycle. By the latter we mean the occurrence of a first-order process with a rate constant of at least 100 sec^{-1}.

It was necessary to state the simplest configuration-type model and to stress that there is no concrete evidence for such a model in order to avoid a misinterpretation of the kinetic scheme. We consider that the type of model in which the configuration is modulated by binding and dissociation of substrate or products is too naive and apparently incapable of accounting for certain features of muscle. For example, one would expect the rate-limiting step for shortening to be product dissociation from the AM·ADP·P complex but the rate of this step (10–20 sec^{-1}) appears to be much too slow to account for the maximum velocity of shortening (Lymn and Taylor, 1970). A different type of configuration model has been proposed by Harrington (1971) which is not naive and which might be tested by kinetic studies.

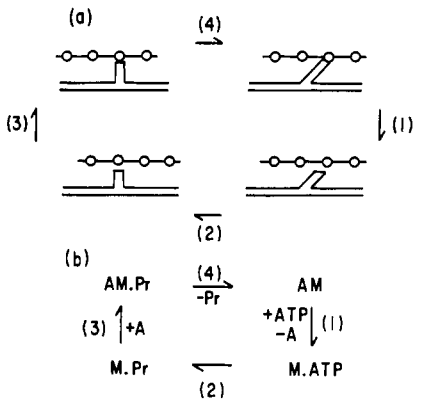

FIGURE 7: (a) Contractile cycle for a single cross bridge. Actin sites which are suitable oriented to interact with a cross bridge are indicated by circles. (b) Steps in chemical mechanism for ATP hydrolysis by actomyosin. Binding of ATP and dissociation of actin is shown as a single step because actin dissociation is very fast following substrate binding. Pr stands for reaction products, ADP, and phosphate.

The kinetic scheme could also be made to fit the general features of the model of Huxley (1957) in which the movement of free bridges is due to thermal energy rather than interaction with substrate.

It is concluded that the kinetic studies allow a beginning to be made in identifying chemical and mechanical steps in the contractile cycle but the available evidence does not yet permit the formulation of a complete quantitative model.

Acknowledgment

We acknowledge the technical assistance of Mrs. Chantal Boyd.

References

Carsten, M. E., and Mommaerts, W. F. H. M. (1963), *Biochemistry 2*, 28.

Eisenberg, E., and Moos, C. (1968), *Biochemistry 7*, 1486.

Eisenberg, E., and Moos, C. (1970), *J. Biol. Chem. 245*, 2451.

Eisenberg, E., Zobel, C. R., and Moos, C. (1969), *Biochemistry 8*, 3186.

Finlayson, B., Lymn, R. W., and Taylor, E. W. (1969), *Biochemistry 8*, 811.

Gergely, J., Martonosi, A., and Gouvea, M. A. (1959), Sulphur in Proteins, Benesch, R., Ed., New York, N. Y., Academic Press.

Gratzer, W. B., and Lowey, S. (1969), *J. Biol. Chem. 244*, 22.

Harrington, W. F. (1971), *Proc. Nat. Acad. Sci. U. S. 68*, 685.
Huxley, A. F. (1957), *Progr. Biophys. 7*, 255.
Huxley, H. E. (1968), *Science 164*, 1356.
Kiely, B., and Martonosi, A. (1968), *J. Biol. Chem. 243*, 2273.
Lymn, R. W., and Taylor, E. W. (1970), *Biochemistry 9*, 2975.
Maruyama, K., and Gergely, J. (1962), *J. Biol. Chem. 237*, 1095.
Pringle, J. W. S. (1967), *Progr. Biophys. 17*, 1.
Taylor, E. W., Lymn, R. W., and Moll, G. (1970), *Biochemistry 9*, 2984.
Tonomura, Y., and Yoshimura, J. (1962), *J. Biochem. (Tokyo) 51*, 259.

Interaction of D-Glucal with *Aspergillus niger* Glucose Oxidase*

M. J. Rogers† and K. G. Brandt‡

ABSTRACT: D-Glucal, a structural analog of D-glucose, is an inhibitor of *Aspergillus niger* glucose oxidase. The inhibition is competitive with respect to D-glucose and uncompetitive with respect to oxygen. In the presence of D-glucal the visible absorption spectrum of the enzyme-bound flavin-adenine dinucleotide in the oxidized form of the enzyme is perturbed. A model is proposed to account for these observations which postulates that D-glucal binds at the active site of the oxidized form of glucose oxidase. The inhibition constant for D-glucal is pH independent over the pH range from 3.8 to 7.5 with an average value of 0.13 M. Comparison of this value with the dissociation constant for the oxidized enzyme–D-glucose complex suggests that D-glucal is not a transition-state analog for glucose oxidase. The pH dependence of the Michaelis constant for 2-deoxy-D-glucose with *A. niger* glucose oxidase was determined in the absence of chloride ion and found to increase at acidic pH by less than twofold between pH 7.0 and 4.0.

Glucose oxidase (β-D-glucose:oxygen oxidoreductase, EC 1.1.3.4) from *Aspergillus niger*, a flavoprotein, catalyzes the oxidation of β-D-glucose by molecular oxygen to give D-glucono-δ-lactone and hydrogen peroxide (Bentley, 1963). The enzyme is highly specific for β-D-glucose, but a few other monosaccharides, *e.g.*, 2-deoxy-D-glucose, D-mannose, and D-galactose, exhibit low activity as substrates (Bentley, 1963). The kinetics of the enzyme-catalyzed reaction have been studied by both steady-state and stopped-flow methods (Gibson *et al.*, 1964; Bright and Gibson, 1967; Nakamura and Ogura, 1968).

Probably due to the remarkable substrate specificity of glucose oxidase, an unreactive competitive inhibitor of the enzyme has not been reported. The availability of such an inhibitor can be of considerable use in studying reaction mechanisms. By using a competitive inhibitor of D-amino acid oxidase, Koster and Veeger (1968) have shown that the mechanism is ordered sequential rather than Ping-Pong. Furthermore, the inhibition constant of a competitive inhibitor should be a simple dissociation constant, in contrast to the Michaelis constant for a substrate which is a complex constant composed of rate constants for both binding and catalytic steps. Consequently, to the extent that inhibitor binding reflects substrate binding, it is possible to separate the effects of pH and other external variables on substrate binding from their effects on subsequent reaction steps.

Lee (1969) has reported that D-galactal (Figure 1A) is a potent inhibitor of β-D-galactopyranosidases. This report prompted us to test D-glucal (Figure 1B) as an inhibitor of glucose oxidase. We have found that D-glucal, a glucose analog, is an inhibitor of *A. niger* glucose oxidase. This paper reports kinetic and spectrophotometric studies of the interaction of D-glucal with glucose oxidase.

Materials and Methods

Lyophilized glucose oxidase from *A. niger* (lots GOP 8AA and GOP 8JA) was obtained from Worthington Biochemical Corp. and used without further purification. Turnover numbers at air saturation extrapolated to infinite D-glucose concentration at 25°, pH 5.6, were 361 sec^{-1} (GOP 8AA) and 293 sec^{-1} (GOP 8JA). These values compare favorably with the value of 356 sec^{-1} calculated for these conditions from the kinetic data of Bright and Gibson (1967) for their enzyme preparations. Assays for contaminating catalase showed only insignificant amounts which did not affect the kinetics. Enzyme concentration, calculated as enzyme-bound FAD[1] concentration, was determined spectrophotometrically at 450 nm using a molar absorptivity of 1.41×10^4 $M^{-1}cm^{-1}$ (Gibson *et al.*, 1964).

D-Glucal was prepared from triacetyl-D-glucal (Aldrich Chemical Co.) based on the procedure of Shafizadeh and Stacey (1952). D-Glucal was obtained as a colorless, hygroscopic solid, mp 58–59° (lit. (Shafizadeh and Stacy, 1952) mp 57–

* From the Department of Biochemistry, Purdue University, Lafayette, Indiana 47907. *Received June 18, 1971.* Supported in part by U. S. Public Health Service Grant No. AM 11470. Journal Paper No. 4466, Purdue University Agricultural Experiment Station, Lafayette, Ind. 47907.

† U. S. Public Health Service predoctoral fellow.

‡ To whom to address correspondence.

[1] Abbreviations used are: FAD, flavin-adenine dinucleotide; (E_T), total concentration of enzyme-bound FAD; E_o, enzyme in which the enzyme-bound FAD is in the oxidized form; E_r, enzyme in which the enzyme-bound FAD is in the reduced form; G, D-glucose; L, D-glucono-δ-lactone; I, D-glucal.